J. Fluid Mech. (1967), *vol.* 28, *part* 3, *pp.* 512–522
Printed in Great Britain

An axisymmetric similarity solution for viscous–transonic nozzle flow

By M. SICHEL AND Y. K. YIN
Department of Aerospace Engineering, University of Michigan, Ann Arbor

(Received 25 July 1966)

An axisymmetric viscous–transonic equation is presented. A nozzle-type similarity solution of this equation has been found, which describes the initial stages in the development of shock waves downstream of a converging–diverging nozzle throat. This solution is an extension of a two-dimensional solution found previously (Sichel 1966). By an appropriate choice of an arbitrary scaling constant solutions were found such that there is essentially a weak normal shock near the axis with effects of wall and shock-wave curvature occurring only at a sufficiently large radius. The upstream and downstream asymptotic behaviour of these viscous–transonic nozzle solutions has been investigated.

1. Introduction

A similarity solution of the inviscid transonic equation describing flow near the throat of a converging–diverging nozzle was found by Tomotika & Tamada (1950) in the two-dimensional case and by Tomotika & Hasimoto (1950) in the axisymmetric case. These solutions describe both the symmetrical Taylor flow with subsonic velocities upstream and downstream of the throat and the asymmetrical subsonic–supersonic Meyer flow, but do not permit a smooth transition between the two types of flow. Since this transition is accompanied by the formation of shock waves downstream of the nozzle throat this difficulty appears due to the neglect of viscous effects. If the longitudinal or compressive viscosity and the thermal conductivity are taken into account the inviscid transonic equation should be replaced by a 'viscous–transonic' equation (Cole 1949; Sichel 1963; Szaniawski 1963; Ryzhov & Shefter 1964). Sichel (1966) found nozzle-type similarity solutions of the two-dimensional viscous–transonic equation that do permit the smooth transition from the Taylor to the Meyer type of flow and display the initial stages in shock-wave formation downstream of the nozzle throat. An axisymmetric viscous–transonic nozzle solution has also been found and is the main subject of the present paper.

2. The axisymmetric nozzle solution

The viscous–transonic equation for the axisymmetric flow of a perfect gas can be shown to be

$$U_{XXX} - (U^2)_{XX} + (U_R/R) + U_{RR} = 0, \tag{1}$$

and, since the flow is irrotational to the order of approximation used in deriving (1),

$$U_R = V_X. \tag{2}$$

In these equations X and R are dimensionless axial and radial co-ordinates and U and V are the corresponding dimensionless velocities. Equations (1) and (2) are derived from the full Navier–Stokes equations by a simultaneous co-ordinate stretching and series expansion, and since the derivation is almost identical to that of the two-dimensional viscous–transonic equation (Sichel 1963) the details will not be reproduced here. Without the third-order viscous term (1) is the same as the inviscid axisymmetric transonic equation (Guderley 1962); without the term U_R/R and with R replaced by Y, (1) becomes the two-dimensional viscous–transonic equation.

The stretched dimensionless co-ordinates X and R, and the corresponding velocities U and V are related to dimensional co-ordinates $\bar{x}$, $\bar{r}$, and velocities $\bar{u}$, $\bar{v}$ by

$$\left.\begin{aligned} X &= A(\bar{x}/\hat{\eta}), \quad R = [\tfrac{1}{2}(\gamma+1)]^{\frac{1}{2}}\epsilon^{\frac{1}{2}}A(\bar{r}/\hat{\eta}), \\ (\bar{u}/a^*) &= 1+\epsilon U, \quad (\bar{v}/a^*) = \epsilon^{\frac{3}{2}}[\tfrac{1}{2}(\gamma+1)]^{\frac{1}{2}}V, \end{aligned}\right\} \tag{3}$$

where

$$A = \tfrac{1}{2}(\gamma+1)\,[1+(\gamma-1)/Pr'']^{-1}.$$

In (3) a^* is the critical speed of sound while ϵ is a small parameter proportional to the maximum deviation of (u/a^*) from the sonic value. The characteristic length $\hat{\eta}$ is equal to $(\mu^{*\prime\prime}/\epsilon\rho^* a^*)$, which is of the order of the thickness of a weak shock. μ'' is the compressive or longitudinal viscosity (Hayes 1958) while ρ is the density, and the asterisk refers to conditions at the sonic point. The Prandtl number Pr'' is based on the viscosity μ'' and is assumed constant. The relations between the deviations of the pressure, density, and temperature from their critical values and the velocity perturbation U are identical to those within an acoustic wave (Sichel 1963).

The transformation

$$\left.\begin{aligned} U &= Z(S)+2\sigma^2R^2, \\ S &= X+\sigma R^2, \end{aligned}\right\} \tag{4}$$

which was also used by Tomotika & Hasimoto (1950), reduces the axisymmetric viscous–transonic equation to the ordinary differential equation

$$Z'''-2ZZ''-2(Z'-\omega_1\sigma)(Z'+\omega_2\sigma) = 0, \tag{5}$$

where

$$\omega_1 = \sqrt{5}+1, \quad \omega_2 = \sqrt{5}-1.$$

The flow described by (4) can be considered to be a nozzle flow by choosing one of the stream-tubes as the nozzle wall. $Z(S)$ will be the value of U on the nozzle axis $R = 0$. The arbitrary constant σ is related to the streamline curvature and will be discussed further below.

Except for the value of the constants ω_1 and ω_2, (5) is identical to the ordinary differential equation considered in the two-dimensional case; therefore the properties of (5) are similar to those of the two-dimensional equation, which has been discussed in detail by Sichel (1966). As before the inviscid solutions

$$Z = \omega_1\sigma(S-b), \tag{6a}$$

$$Z = -\omega_2\sigma(S-b) \tag{6b}$$

also satisfy the viscous equation, and (6a) represents the inviscid Meyer-type subsonic–supersonic accelerating flow. The arbitrary constant b locates the sonic

point $Z = 0$. Again the behaviour of solutions of (5) in the Z'', Z', Z phase space can be established by studying the two-dimensional trajectories obtained when Z is held constant, and there will be singularities where the inviscid solutions pierce the (Z = constant)-planes. The point $Z' = \omega_1 \sigma$, $Z'' = 0$ will be a saddle-point for all Z while the point $Z' = -\omega_2 \sigma$, $Z'' = 0$ will be an unstable node, an unstable spiral point, a stable spiral point and a stable node respectively for Z corresponding to the ranges

$$Z > [2\sigma(\omega_1+\omega_2)]^{\frac{1}{2}}; \quad [2\sigma(\omega_1+\omega_2)]^{\frac{1}{2}} > Z > 0; \quad 0 > Z > -[2\sigma(\omega_1+\omega_2)]^{\frac{1}{2}};$$
$$-[2\sigma(\omega_1+\omega_2)]^{\frac{1}{2}} > Z.$$

Thus any solution starting near the inviscid accelerating solution will diverge from it for all Z; however, some of these solutions pass through a maximum and then asymptotically approach the inviscid decelerating solution.

Numerical solutions of (5) representing stages in the transition from the Taylor to the Meyer type of flow are shown in figures 1 (*a*), (*b*) and (*c*) for $\sigma = 1{\cdot}0$, $0{\cdot}5$ and $0{\cdot}1$, and were obtained by choosing initial values very close to the accelerating inviscid solution and lying on the directrix of the saddle-point in the corresponding (Z = constant)-plane. Integrating (5) once yields

$$Z'' - 2(ZZ') + 2\sigma(\omega_1 - \omega_2)\, Z + 2\omega_1\omega_2\sigma^2 S = C_1, \tag{7}$$

and initial conditions $Z(S_0)$, $Z'(S_0)$ and $Z''(S_0)$ were chosen so that the constant $C_1 = 0$, for then it follows from (7) that the transitional solutions will be asymptotic to $Z = -\omega_2 \sigma S$ as $S \to +\infty$ and to $Z = \omega_1 \sigma S$ as $S \to -\infty$.

In figure 1, Z represents the nozzle centreline velocity distribution so that $Z = 0$ corresponds to the sonic point. As in the two-dimensional case, figure 1 shows the gradual development of what appears to be a shock wave as the maximum of Z increases beyond the sonic value. With increasing $Z_{\max}$ the velocity gradient steepens in the region of transition from supersonic to subsonic flow. The expansion scheme which provides the basis for the derivation of the viscous–transonic equation will be valid only if U, and hence Z, are $O(1)$; therefore the solutions with $Z_{\max}$ greater than $2{\cdot}0$ to $3{\cdot}0$, while of interest with regard to the overall behaviour of (5), cannot accurately represent the transition from the Taylor to the Meyer flow. As the parameter σ decreases the supersonic–subsonic transition shifts to larger values of S for a given value of $Z_{\max}$. With $\sigma = 0{\cdot}1$ these transitions appear to closely approximate a normal shock wave with almost uniform upstream and downstream flow.

Weak normal shock waves are to order ϵ symmetrical with respect to the sonic point for, if the upstream velocity $\bar{u}_1/a^* = 1 + \epsilon U_1$, the velocity $\bar{u}_2/a^*$ downstream of the shock will be $1 - \epsilon U_1$. Supposing $Z_{\max}$ to be U_1 it can be seen that, as in two dimensions, nozzle flow transitions overshoot the corresponding downstream Hugoniot value $U_2 = -Z_{\max}$. For subsonic Taylor-type flows with $S < 0$, Z diverges from the inviscid solution $Z = \omega_1 \sigma S$ very slowly, but for large positive values of S the solution $Z(S)$ very rapidly deviates from the inviscid solution. On the other hand, even for $S \gg 1$ the solutions approach the decelerating inviscid solution $Z = -\omega_2 \sigma S$ very gradually. This behaviour can be verified analytically

by studying the asymptotic behaviour of Z near the two inviscid solutions as discussed below.

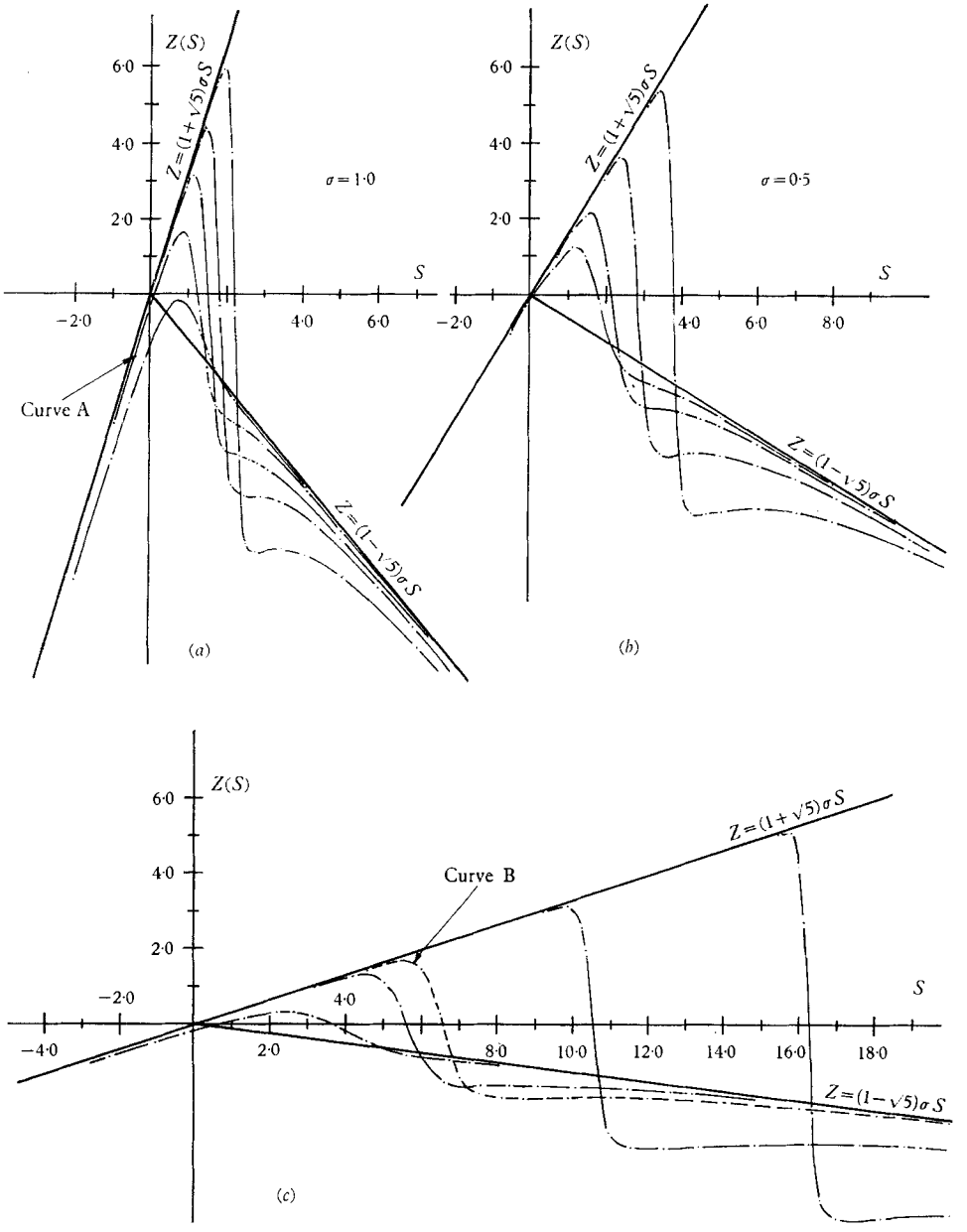

FIGURE 1 (*a*), (*b*), (*c*). Numerical solutions of the equation

$$Z'' - 2ZZ''' - 2(Z' - \omega_1\sigma)(Z' + \omega_2\sigma) = 0.$$

3. Asymptotic behaviour

Although (5) could only be solved numerically it is possible to determine analytically the asymptotic behaviour of $Z(S)$ where it lies near the inviscid solutions. Thus from

$$Z = \omega_1 \sigma S + \zeta_1, \quad Z = -\omega_2 \sigma S + \zeta_2, \tag{8}$$

it follows that the perturbations ζ_1, $\zeta_2 \ll 1$ respectively where Z asymptotically approaches the inviscid solutions $Z = \omega_1 \sigma S$ and $Z = -\omega_2 \sigma S$. Substituting (8) into (7) for Z and dropping terms of $O(\zeta_1^2)$ and $O(\zeta_2^2)$ then yields the following linear differential equations for ζ_1 and ζ_2:

$$\left.\begin{aligned} \zeta_1'' - 2\omega_1 \sigma S \zeta_1' - 2\omega_2 \sigma \zeta_1 &= 0, \\ \zeta_2'' + 2\omega_2 \sigma S \zeta_2' + 2\omega_1 \sigma \zeta_2 &= 0. \end{aligned}\right\} \tag{9}$$

Equations (9) are readily reduced to Weber's equation and have the solutions

$$\left.\begin{aligned} \zeta_1 &= e^{\frac{1}{2}\omega_1 \sigma S^2}\{C_3 U[(\omega_2/\omega_1) - \tfrac{1}{2}, S] + C_4 V[(\omega_2/\omega_1) - \tfrac{1}{2}, S]\}, \\ \zeta_2 &= e^{-\frac{1}{2}\omega_2 \sigma S^2}\{C_5 U[(\omega_1/\omega_2) - \tfrac{1}{2}, S] + C_6 V[(\omega_1/\omega_2) - \tfrac{1}{2}, S]\}, \end{aligned}\right\} \tag{10}$$

where $U(a, S)$, $V(a, S)$ are parabolic cylinder functions of S with parameter a as defined and tabulated by Miller (1964); and C_3, C_4, C_5 and C_6 are arbitrary constants.

The numerical results for $Z(S)$ (figure 1) indicate a difference in the behaviour of ζ_1 and ζ_2 for large S and this can be verified from (10). Thus, using the asymptotic expansion for U and V as $S \to +\infty$ (Miller 1964) and keeping only the largest term in each expansion, it follows that

$$\left.\begin{aligned} \zeta_1(S) &\sim C_3 S^{-\omega_2/\omega_1}[1 + O(1/S^2)] + C_4 S^{(\omega_2/\omega_1)-1} e^{\omega_1 \sigma S^2}[1 + O(1/S^2)], \\ \zeta_2(S) &\sim C_5 S^{(\omega_1/\omega_2)-1} e^{-\omega_2 \sigma S^2}[1 + O(1/S^2)] + C_6 S^{-\omega_1/\omega_2}[1 + O(1/S^2)]. \end{aligned}\right\} \tag{11}$$

For a given S_0 the choice of $\zeta_1(S_0)$, $\zeta_2(S_0)$, $\zeta_1'(S_0)$ and $\zeta_2'(S_0)$ determines the constants in (10). Asymptotic expressions for the derivatives $\zeta_1'(S)$ and $\zeta_2'(S)$ are thus required and can be determined by differentiating (9) and determining the asymptotic behaviour of the solution of the resultant Weber's equation for ζ_1' and ζ_2' with the result that, as $S \to \infty$,

$$\left.\begin{aligned} \zeta_1'(S) \sim{}& -(\omega_2/\omega_1) C_3 S^{-[(\omega_2/\omega_1)+1]}[1 + O(1/S^2)] \\ &+ 2\omega_1 \sigma C_4 S^{\omega_2/\omega_1} e^{\omega_1 \sigma S^2}[1 + O(1/S^2)], \\ \zeta_2'(S) \sim{}& -2\omega_2 C_5 \sigma S^{\omega_1/\omega_2} e^{-\omega_2 \sigma S^2}[1 + O(1/S^2)] \\ &- (\omega_1/\omega_2) C_6 S^{-[(\omega_1/\omega_2)+1]}[1 + O(1/S^2)]. \end{aligned}\right\} \tag{12}$$

The need to differentiate the asymptotic expansions (11) directly, a procedure sometimes not valid (De Bruijn 1958), is thereby avoided. The form of (12) is such that C_3, C_4, C_5 and C_6 are the same as the constants in (11), and (11) can be recovered by integrating the asymptotic expressions (12). The constants in (10) can now be evaluated with the result that

$$\zeta_1(S) = D(S/S_0)^{-\omega_2/\omega_1} + E(S/S_0)^{(\omega_2/\omega_1)-1} \exp\{\omega_1 \sigma (S^2 - S_0^2)\}, \tag{13a}$$

$$\zeta_2(S) = F(S/S_0)^{(\omega_2/\omega_1)-1} \exp\{-\omega_2 \sigma (S^2 - S_0^2)\} + G(S/S_0)^{-\omega_1/\omega_2}, \tag{13b}$$

with

$$D = \left(\zeta_{10} - \frac{\zeta'_{10}}{2\omega_1 \sigma S_0}\right)\left(1 + \frac{\omega_2}{2\omega_1^2 \sigma S_0^2}\right)^{-1},$$

$$E = \frac{1}{2\omega_1 \sigma}\left(\frac{\zeta_{10}\omega_2}{\omega_1 S_0^2} + \frac{\zeta'_{10}}{S_0}\right)\left(1 + \frac{\omega_2}{2\omega_1^2 \sigma S_0^2}\right)^{-1},$$

$$F = -\frac{1}{2\omega_2 \sigma}\left(\frac{\zeta_{20}\omega_1}{\omega_2 S_0^2} + \frac{\zeta'_{20}}{S_0}\right)\left(1 - \frac{\omega_1}{2\sigma\omega_2^2 S_0^2}\right)^{-1},$$

$$G = \left(\zeta_{20} + \frac{\zeta'_{20}}{2\sigma\omega_2 S_0}\right)\left(1 - \frac{\omega_1}{2\sigma\omega_2^2 S_0^2}\right)^{-1},$$

where the subscript zero indicates values at $S = S_0$.

(13*a*) shows that, except for the special case $E = 0$, $\zeta_1(S)$ increases very rapidly for $S > S_0$ as do the numerical solutions in figure 1. The term $(S/S_0)^{-\omega_2/\omega_1}$ dies out with increasing S and so will have little effect upon ζ_1. (13*a*) is consistent with the saddle-point behaviour near $Z = \omega_1 \sigma S$ discussed previously, for $\zeta_1(S)$ will tend to zero with increasing S only in the special case

$$\zeta_{10} = -(\omega_1/\omega_2) S_0 \zeta'_{10}$$

for which $E = 0$, otherwise ζ_1 increases with increasing S. As S decreases, i.e. $S < S_0$, the exponential part of (13*a*) decays rapidly but the $(S/S_0)^{-\omega_2/\omega_1}$ term increases unless $D = 0$. The special solutions $D = 0$ and $E = 0$ thus correspond to solutions lying on the directrices of the saddle-point, and the solution which approaches $Z = \omega_1 \sigma S$ as S decreases is clearly the one with $D = 0$. The numerical integrations were started near $Z = \omega_1 \sigma S$ and at points lying on the directrix of the solution diverging from the point $Z' = \omega_1 \sigma$, $Z'' = 0$, in the appropriate (Z = constant)-plane, a procedure equivalent to choosing $D = 0$. Nevertheless, because of round-off errors the solutions always diverge from the inviscid solution when integrating backward from the starting point.

Both terms of the expansion for $\zeta_2(S)$, (13*b*), tend to zero with increasing S in accordance with the fact that the point $Z' = \omega_2 \sigma$, $Z'' = 0$ is a stable node in the (Z = constant)-plane for $Z < -2\sigma^{\frac{1}{2}}(\omega_2 + 1)^{\frac{1}{2}}$. The exponential term decays rapidly when $S > S_0$ so that $\zeta_2(S)$ will be dominated by $(S/S_0)^{-\omega_1/\omega_2}$ and so approaches the inviscid solution $Z = -\omega_2 \sigma S$ relatively slowly as do the numerical solutions in figure 1.

The asymptotic expansions for $U(a, S)$ and $V(a, S)$ presented by Miller (1964) are not valid for $S < 0$; however, by using the expansion for $U(a, -S)$ (Whittaker & Watson 1952) together with appropriate recursion formulas for U and V and redefining the standard solution for Weber's equation in the cases $S < 0$, (13*a*) and (13*b*) for ζ_1 and ζ_2 can be shown to be valid for $S \to -\infty$. Now, however, for $S > S_0$, $S^2 < S_0^2$ so that the exponential term in (13*a*) decays rapidly while the power term $(S/S_0)^{-\omega_2/\omega_1}$ increases. Again in accordance with the numerical curves, Z deviates from the inviscid solution very slowly with increasing S as $S_0 \to -\infty$, particularly since $\omega_2/\omega_1 = 0{\cdot}382$ in the axisymmetric case.

From the inviscid solution of Tomotika & Hasimoto (1950) for Z it can be shown that $\zeta_1 \sim |S|^{-\omega_2/\omega_1}$ and $\zeta_2 \sim |S|^{-\omega_1/\omega_2}$ as $S \to \pm\infty$. The exponential terms in (13*a*) and (13*b*), which account for the difference in the behaviour of the subsonic and supersonic solutions, thus reflect the effects of viscosity.

The discussion of asymptotic behaviour given above is fully applicable to the two-dimensional case (Sichel 1966) provided the two-dimensional values ω_1, $\omega_2 = 2{\cdot}0,\ 1{\cdot}0$ are used in place of the axisymmetric values $\omega_1,\ \omega_2 = (\sqrt{5}+1),\ (\sqrt{5}-1)$.

4. Nature of the flow

To compute the streamlines corresponding to the solutions in figure 1 the vertical velocity, V, must be known, and can be determined from the irrotationality condition and (7) with the result

$$V = 2\sigma RZ + 4\sigma^2 RX + \tfrac{1}{2}\omega_1\omega_2\sigma^3 R^3 + \tfrac{1}{2}C_1 R + C_2 R^{-1}. \tag{14}$$

The arbitrary constant C_2 is taken to be zero since only solutions with finite V on the axis $R = 0$ are of interest. The constant C_1 merely translates the origin of S and so, for convenience, will be taken as zero. Unlike (5) and the foregoing asymptotic analysis, (14) cannot be extended to the two-dimensional case. To the present order of approximation the streamlines satisfy the differential equation

$$d\bar{r}_S/d\bar{x} = \epsilon^{\frac{3}{2}}[(\gamma+1)/2]^{\frac{1}{2}}\, V, \tag{15}$$

where $\bar{r}_S(\bar{x})$ is the variation of the radius $\bar{r}$ along any given streamline. In terms of $R_S(x)$, (15) becomes

$$dR_S/dX = \tfrac{1}{2}\epsilon^2(\gamma+1)\,V. \tag{16}$$

The significance of ϵ^2 in (16) and the relation between solutions in the $(X$–$R)$- and physical $(\bar{x}$–$\bar{r})$-plane are the same as in the two-dimensional case (Sichel 1966).

Generally it is desirable to specify the ratio of throat radius $\bar{r}_t$ to the radius of curvature of the nozzle wall streamline. To the present order of approximation the streamline curvature, $\bar{L}^{-1}$, at any point in the flow is given by

$$\frac{1}{\bar{L}} = \frac{d^2 r_S}{dx^2} = \epsilon^{\frac{3}{2}}\left(\frac{\gamma+1}{2}\right)^{\frac{1}{2}}\frac{dV}{d\bar{x}} = 2\epsilon^{\frac{3}{2}}\left(\frac{\gamma+1}{2}\right)^{\frac{1}{2}}\frac{A}{\hat{\eta}}\,\sigma R(Z' + 2\sigma), \tag{17}$$

where $\bar{L}$ is the streamline radius of curvature. For most cases of interest the transition from supersonic to subsonic flow occurs well beyond the throat; hence, the flow in the immediate vicinity of the throat follows the inviscid solution, $Z = \omega_1\sigma S$, so that $(\bar{L}/\hat{\eta})$ is given by

$$(L/\hat{\eta}) = \{2\epsilon^{\frac{3}{2}}[\tfrac{1}{2}(\gamma+1)]^{\frac{1}{2}} R\sigma^2(\omega_1+2)\}^{-1}. \tag{18}$$

With the ratio $\bar{r}_t/\bar{L}_t$ of throat radius to wall radius of curvature fixed at β, the throat radius $\bar{r}_t$ will then be

$$\bar{r}_t = \frac{\hat{\eta}\beta^{\frac{1}{2}}}{A\epsilon\sigma(\gamma+1)(\omega_1+2)^{\frac{1}{2}}}. \tag{19}$$

The axial throat co-ordinate $\bar{x}_t$ is derived using the condition $V = 0$ at the throat as in the two-dimensional case (Sichel 1966).

Isotachs, or lines of constant speed in the $(\bar{r}$–$\bar{x})$-plane correspond to curves along which U is constant to the present order of approximation, and so can be

determined from (4) and the numerical solutions for Z. In the region of inviscid flow the velocity perturbations ϵU and $\epsilon^{\frac{3}{2}}[\frac{1}{2}(\gamma+1)]^{\frac{1}{2}} V$ are given by

$$\epsilon U = \frac{\bar{u}}{a^*} - 1 = \frac{\omega_1 \beta^{\frac{1}{2}}}{[(\gamma+1)(\omega_1+2)]^{\frac{1}{2}}} \xi + \tfrac{1}{2}\beta\eta^2, \tag{20}$$

$$\epsilon^{\frac{3}{2}}[\tfrac{1}{2}(\gamma+1)]^{\frac{1}{2}} V = \frac{\bar{v}}{a^*} = \beta\eta\xi + \frac{2(\omega_1+1)\beta^{\frac{3}{2}}[\frac{1}{2}(\gamma+1)]^{\frac{1}{2}}}{[2(\omega_1+2)]^{\frac{3}{2}}} \eta^3, \tag{21}$$

when $\bar{r}_t$ is chosen as a reference length so that

$$\xi = (\bar{x}/\bar{r}_t), \quad \eta = (\bar{r}/\bar{r}_t).$$

Integration of (15) using (21) for $\bar{v}/a^*$ then yields the following expression for the wall streamline in the portion of the flow where $Z = \omega_1 \sigma S$:

$$\frac{\bar{r}}{\bar{r}_t} = \eta = \exp(\tfrac{1}{2}\beta\xi^2)\left[\exp(\beta\xi_t^2) - \frac{4(\omega_1+1)\beta^{\frac{3}{2}}[\frac{1}{2}(\gamma+1)]^{\frac{1}{2}}}{[2(\omega_1+2)]^{\frac{3}{2}}} \int_{\xi_t}^{\xi} \exp(\beta\lambda^2)\, d\lambda\right]^{-\frac{1}{2}}. \tag{22}$$

With ξ_t, the throat co-ordinate, given by

$$\xi_t = (x_t/r_t) = -\frac{2\beta^{\frac{1}{2}}(\omega_1+1)[\frac{1}{2}(\gamma+1)]^{\frac{1}{2}}}{[2(\omega_1+2)]^{\frac{3}{2}}}, \tag{23}$$

(22) shows that $\eta \to \infty$ for sufficiently large ξ, but for those solutions with Z and $U \sim O(1)$ transition to subsonic flow occurs long before η diverges to infinity. Once Z deviates from $Z = \omega_1 \sigma S$, (15) can only be integrated numerically.

The relation between the arbitrary constant σ and the nozzle flow field can be seen from (18) and (19). With ϵ, $\hat{\eta}$ and γ fixed, the streamline radius of curvature $\bar{L}$ varies inversely with σ^2 for a given fixed radius R, and the velocity gradient of the inviscid solutions ahead of and behind the viscous transition decreases, as is evident from figure 1. As discussed previously with this decrease in velocity gradient the viscous transition, at least on the nozzle centreline, approaches the Taylor (1910) shock transition. For fixed β and ϵ the nozzle throat radius $\bar{r}_t$ varies inversely with σ, (19).

Typical isotach contours and streamlines for $\sigma = 1{\cdot}0$ and $0{\cdot}1$, corresponding to curves A and B in figures 1 (*a*) and 1 (*c*), are shown in figures 2 (*a*) and 2 (*b*) in the (ξ–η)-plane. Figures 2 (*a*) and 2 (*b*) have been drawn using numerical solutions with the same peak value of Z, and with wall streamlines corresponding to $\beta = 0{\cdot}21$ as in the paper by Tomotika & Hasimoto (1950). Since the flow is axisymmetric the isotachs are really the intersections of constant-speed surfaces with planes through the nozzle axis.

The strange shape of the isotachs downstream of the region of rapid deceleration in figure 1 (*b*) results from the slight increase in $Z(S)$ immediately behind the shock-like transition. The $\sigma = 0{\cdot}1$ wall streamline has a second minimum some distance downstream of the supersonic–subsonic transition; however, for streamlines with β sufficiently small this second throat disappears. An inherent property of similarity solutions, such as presented here, is, of course, the inability to specify streamline shapes *a priori*. The shock-like nature of the supersonic–subsonic transition is clearly indicated, particularly in the case of $\sigma = 0{\cdot}1$.

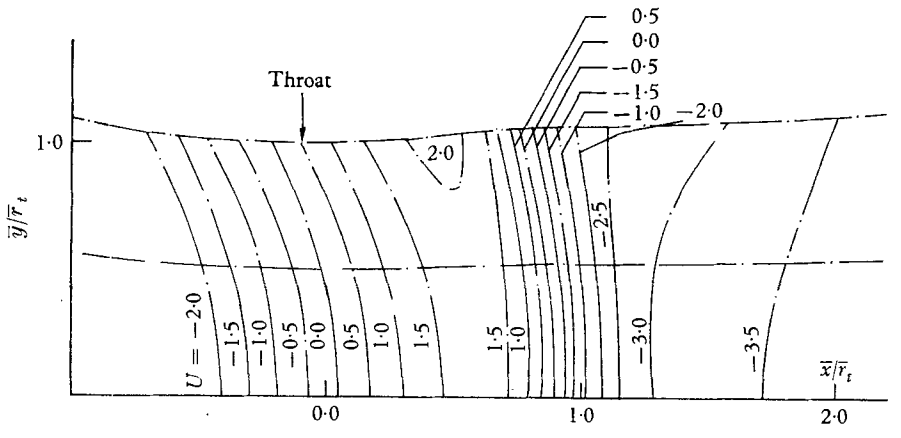

$\epsilon = 0{\cdot}1 \quad \gamma = 1{\cdot}4 \quad \bar{U}/a^* = \epsilon U \quad \beta = \bar{r}_t/\bar{L}_t = 0{\cdot}21 \quad \sigma = 1$

FIGURE 2(*a*). Isotachs and streamlines corresponding to curve A in figure 1(*a*).

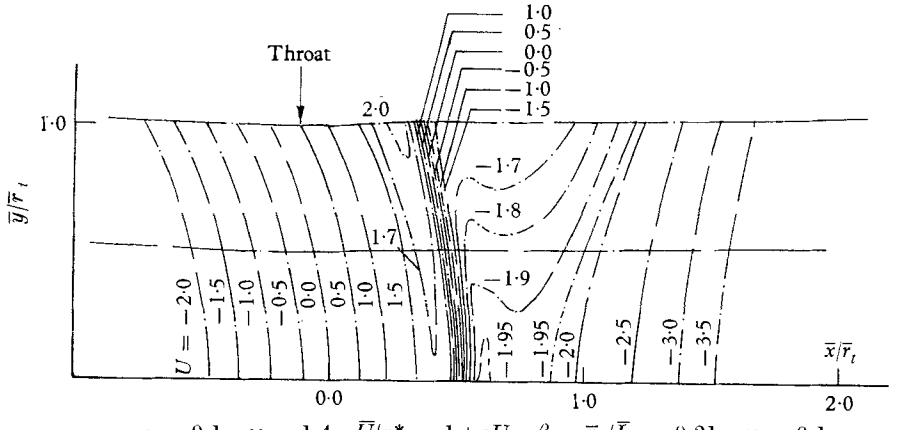

$\epsilon = 0{\cdot}1 \quad \gamma = 1{\cdot}4 \quad \bar{U}/a^* = 1+\epsilon U \quad \beta = \bar{r}_t/\bar{L}_t = 0{\cdot}21 \quad \sigma = 0{\cdot}1$

FIGURE 2(*b*). Isotachs and streamlines corresponding to curve B in figure 1(*c*).

5. Discussion

The axisymmetric nozzle similarity solutions are quite similar to the two-dimensional solutions found previously (Sichel 1966). In the present case the asymptotic behaviour of the solutions for the centreline velocity Z has been investigated, and the difference in the behaviour of the numerical solutions in regions of subsonic and supersonic flow has been verified analytically. The effect of the parameter σ upon the nozzle solutions has been examined. Figure 2(*b*) shows that when $\sigma \ll 1$ solutions are obtained such that there is essentially a weak normal shock near the axis with effects of the wall and shock curvature occurring only for sufficiently large $\bar{r}$ as was anticipated previously.

The authors would like to express their appreciation to the Army Research Organization in Durham, N.C., for their support of this work under Contract DA-31-124-ARO-D-276.

REFERENCES

COLE, J. 1949 Problems in transonic flow. Ph.D. Thesis, California Institute of Technology.

DEBRUIJN, N. G. 1958 *Asymptotic Methods in Analysis.* Amsterdam: North-Holland Publishing Company.

GUDERLEY, K. G. 1962 *The Theory of Transonic Flow.* Reading: Addison Wesley.

HAYES, W. D. 1958 *Fundamentals of Gas Dynamics*, §D. Princeton University Press.

MILLER, J. C. P. 1964 Parabolic cylinder functions, chapter 19. *Handbook of Mathematical Functions* (ed. M. Abramowitz and I. A. Stegun). U.S. National Bureau of Standards, Washington, D.C.

RYZHOV, O. S. & SHEFTER, G. M. 1964 *Prikl. Mat. i Mekh.* **28**, 996.

SICHEL, M. 1963 *Phys. Fluids* **6**, 653.

SICHEL, M. 1966 *J. Fluid Mech.* **25**, 769.

SZANIAWSKI, A. 1963 *Archiwum Mechaniki stosowanej*, **15**, 904.

TAYLOR, G. I. 1910 *Proc. Roy. Soc.* A, **84**, 371.

TOMOTIKA, S. & HASIMOTO, Z. 1950 *J. Math. Phys.* **29**, 105.

TOMOTIKA, S. & TAMADA, K. 1950 *Quart. Appl. Math.* **7**, 381.

WHITTAKER, E. T. & WATSON, G. N. 1952 *A Course of Modern Analysis*, 4th ed. Cambridge University Press.